INTRODUCTION

In this paper we shall discuss some of the aspects of the difficult problem encountered when trying to describe quantitatively the structure of lifted laminar jet diffusion flames. We shall consider, in particular, the role that triple flames have in determining the ignition of diffusion flames by localized heat sources, and on the lift-off distance of the flames, when the triple flame generated by the external heat source does not travel all the way up to the injector rim.

A significant amount of work has been carried out on the structure of edge and triple flames, but we begin by acknowledging here the contribution of Forman Williams (1971), with his paper in the *Annual Review of Fluid Mechanics*, in calling the attention of the scientific community to the role that the large sensitivity with temperature of the overall reaction has in the combustion phenomena. In particular, in his 1971 seminal paper he discusses the triple flame observed experimentally by Phillips (1965), showing that its structure is a consequence of the large activation energy of the reaction.

Triple flames, also known as tribrachial flames, or the more general edge flames, play an important role in diffusion flame attachment and lift-off (Liñán, 1988, 1994; Takahashi and Katta, 1990; Takahashi et al., 1998; Fernández et al., 2000; Buckmaster and Weber, 1996), and in the ignition and reignition processes of nonpremixed systems (Réveillon et al., 1995; Vervisch and Poinsot, 1998; Favier and Vervisch, 1998; Peters, 2000). Such flames have been studied experimentally (Kioni et al., 1993; Shay and Ronney, 1998; Azzoni et al., 1999; Santoro et al., 2000; Aggarwal et al., 2001), theoretically (Dold, 1989; Dold et al., 1991; Hartley and Dold, 1991), and numerically (Ruetsch et al., 1995; Daou and Liñán, 1998; Boulanger and Vervisch, 2003) by several authors, due to the role they play as transient laminar flamelets in partially premixed systems (Peters, 1986). The triple flame encountered in

unsteady or parallel mixing layers, described by Liñán and Crespo (1976), when initiated at high enough initial temperatures by the heat release due to the reaction, is not associated with the upstream heat conduction of ordinary edge flames.

The first analysis of the two-dimensional structure of a triple flame is due to Dold (1989) and coworkers (Dold et al., 1991; Hartley and Dold, 1991), who used a constant density model with a single-step chemical reaction with large activation energy. The analysis, restricted to the equidiffusive case, showed that the triple-flame propagation speed depends on the transverse mixture fraction gradient, having a value that, in the constant density scenario, is bounded above by the maximum adiabatic laminar flame speed of the system. The analysis of triple flames was later extended to non-unity Lewis numbers by Daou and Liñán (1998), still using the constant density approximation.

Using a different approach, Buckmaster (1996) developed a simplified one-dimensional model containing some of the key physical ingredients of the problem as a tool for improving the understanding of edge-flames. The one-dimensional model included non-unity fuel Lewis number and finite-rate chemistry leading to an overall Damköhler number *Da*. Despite its simplicity, the one-dimensional model predicts flames with advancing, retreating, or stationary edges depending on *Da*. Later on, still in this simplified context, Nayagam and Williams (2002) showed that, for sufficiently large Lewis numbers, both advancing and receding flame edges may exist for a given value of *Da*.

The first analysis of the effects of heat release on the propagation velocity of triple flames is due to Ruetsch et al. (1995). Due to the flow redirection ahead of the curved triple-flame front, the velocity component along the stoichiometric surface was seen to decrease from its value far upstream the triple flame to a minimum value, just upstream of the flame, close to the planar laminar flame speed. This is in agreement with the experimental observation that the propagation velocities of triple flames are significantly higher than the adiabatic laminar burning velocity for the corresponding premixed stoichiometric fuel-air mixture (Phillips, 1965; Kioni et al., 1993). The analysis of Ruetsch et al. (1995) was later generalized by Favier and Vervisch (1998, 2001), who studied unsteady effects at the edge of a diffusion flame perturbed by vortices. Small but finite heat release effects were also accounted for in the parabolic flame model of Ghosal and Vervisch (2000). There is a more recent attempt by Boulanger and Vervisch (2003) to analyze

numerically the effects of heat release in axisymmetric lifted laminar diffusion flames. For further references on triple- and edge-flame propagation the reader is referred to the recent review paper by Buckmaster (2002).

The problem of lifted laminar jet diffusion flames has also been considered in the literature, beginning with the work of Chung and Lee (1991) and Lee and Chung (1997), who analyzed their experimental results in terms of the upstream velocity and concentration distributions provided by the Schlichting far-field self-similar description of laminar jets. They equate the upstream velocity at the stoichiometric surface to an assumed triple flame velocity. Revuelta et al. (2002) showed how this analysis could be generalized to account for the non-self-similarity of the upstream velocity and concentration profiles when the lifted flame is not in the far field; but they neglect also the effects of the thermal expansion when determining the flame front propagation.

The first numerical study of a lifted round jet diffusion flame, accounting for thermal expansion effects, is due to Plessing et al. (1998); this was carried out with a detailed reaction mechanism for a jet of methane, diluted with nitrogen, with an outer lean methane-air mixture. A more recent numerical and experimental study of lifted laminar jet diffusion flames, in microgravity or under normal gravity, has been carried out by Walsh et al. (2004) for pure or diluted methane jets with coflowing air; a detailed kinetic scheme was also used in the analysis. We must also acknowledge here the tour de force represented by the direct numerical simulation (DNS) carried out by Mizobuchi et al. (2002) of a lifted turbulent hydrogen jet diffusion flame.

The purpose of the present paper is to formulate the problem of the description of the lift-off height in laminar vertical jet diffusion flames, for values of the Reynolds number based on the injector radius a and fuel flow velocity U_0 moderately large compared with unity. We shall account for the effects of gravity and for the effects of the velocity U_A of the coflowing air stream.

A thermochemistry parameter that plays an important role is the overall air-to-fuel stoichiometric ratio $S = sY_{F0}/Y_{O_2A}$, defined in terms of the mass fractions Y_{F0} and Y_{O_2A} of fuel and oxygen in the feed streams, and the mass s of oxygen required to burn, with the global reaction, the unit mass of fuel. This parameter, together with the temperature T_0 of the feed streams, which for simplicity in the formulation we shall consider to be equal, determines the stoichiometric flame temperature

$T_s = T_0 + qY_{F0}/[c_p(1+S)]$, with the assumption of a constant value c_p of the specific heat. Also for simplicity in the presentation, we shall consider that the mass diffusivities of all the species are equal to the thermal diffusivity D_T, and that the viscosity μ and the product ρD_T are functions only of the temperature. The Prandtl number $Pr = \mu c_p/k$ will be considered constant.

An important kinetic parameter is the ratio U_0/S_L of the fuel jet velocity to the planar flame velocity S_L of the stoichiometric mixture formed with the unit mass of the fuel stream and a mass S of the air stream. We anticipate that when S is of order unity the flame will be blown off if U_0/S_L rises above a blow-off value $(U_0/S_L)_b$, also of order unity, to be calculated; due to thermal expansion effects this value is larger than 1. When S is large and the coflow velocity ratio U_A/U_0 is small compared with unity, the blow-off value of U_0/S_L is of order S.

We shall formulate the problem of the description of the flow configuration of a lifted jet diffusion flame when the Reynolds number $Re = aU_0/\nu_A$, based on the kinematic viscosity ν_A of the air stream, is large compared with unity, although not so large that the flow ceases to be laminar and steady. We shall consider the feed streams to come out normal from a porous wall, with a temperature T_0 and uniform velocities U_0 and U_A. The analysis begins with the distinguished limiting case when the fuel stream is diluted so that S is reduced to values of order unity, with the ratios U_0/S_L and U_A/U_0 also taken to be of order unity. Separate consideration will be given to the practical case $S \gg 1$ with $U_A/U_0 \ll 1$ and $S^{-1}U_0/S_L \sim 1$, when the flame may be lifted in the far field, at distances from the injector of order $Re\, a\, S$.

When the Reynolds number aU_0/ν_A is large compared with unity the jet is slender with a developing length, $L_d = aRe$, large compared with the injector radius a. If the ratio U_0/S_L is small compared with unity the diffusion flame will be anchored near the injector wall, whereas when U_0/S_L grows to values of order unity, the case considered here, the flame will be lifted to a height $x_l \sim L_d$, or the flame will be blown off for flow velocities such that U_0/S_L is larger than the critical value $(U_0/S_L b)$. When the flame is lifted the flame configuration is as sketched in Figure 1. There is a flame front region of size a where, due to the effects of heat release, the streamlines are significantly deflected from the axial direction. The deflection is strong in the premixed flames, of thickness of order $\delta_L = D_{TA}/S_L \ll la$, and more gradual both upstream and downstream of the premixed flames.

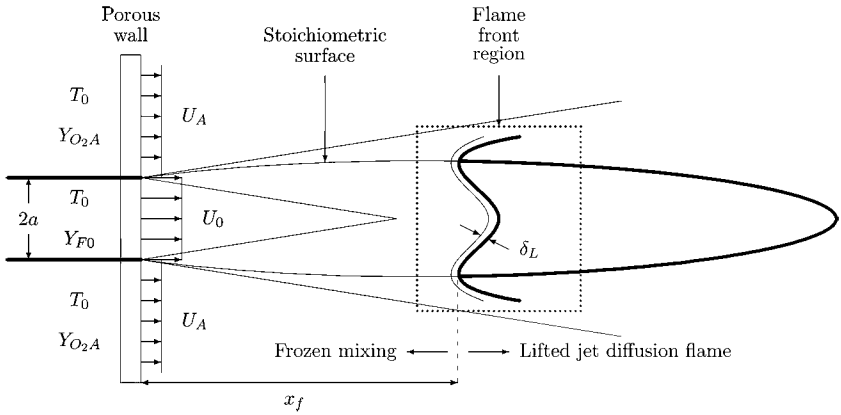

Figure 1. A sketch of a laminar lifted flame in a coflow jet.

Because the effective Reynolds number of the flow in the flame front region is of order a/δ_L, large compared with unity, the viscous and diffusion effects can be neglected in this region, both upstream and downstream of the flame front, but not in the thin premixed flames. The viscous and diffusive terms, associated with the radial derivatives, must also be retained when analyzing the slender regions upstream and downstream of the flame front region. In the following section, we first describe the upstream structure of the jet, required to determine the profiles of velocity and mixture fraction upstream from the flame. The formulation for the numerical description of the flame front region is given next, and is followed by the discussion of some limiting cases and illustrative results. Concluding remarks are offered in the final section. Note that the description of the downstream slender diffusion flame region, not addressed here, would only be necessary if higher-order corrections, due to the effects of the thermal expansion occurring in the diffusion flame region, are sought in the flame front region.

JET STRUCTURE UPSTREAM FROM LIFTED FLAMES

Upstream of the flame front the chemical reaction can be considered frozen. Because the Reynolds number $Re = U_0 a/\nu_A$ is large compared with unity, the jet is slender and can be described using the boundary-layer approximation. The conservation equations will be written in nondimensional form using the scale aRe for the downstream distance, and the jet radius a for the radial distance, leading to $\chi = x/(aRe)$ and $r = r'/a$. On

the other hand, we shall use U_0 and $U_0/Re = \nu_A/a$ as scales to define the dimensionless axial and radial velocity components $u = u'/U_0$ and $v = v'/(U_0/Re)$, while the density ρ will be measured with the density ρ_A of the air stream.

The typical Mach number is in most applications small compared with unity, so that we can neglect the pressure variations in the equation of state and the kinetic energy and viscous dissipation in the energy equation. With these approximations, $T = T_0$ upstream of the flame front region, and the conservation equations for the upward flowing vertical jet take the form

$$\frac{\partial}{\partial \chi}(\rho u) + \frac{1}{r}\frac{\partial}{\partial r}(r\rho v) = 0 \tag{1}$$

$$\rho u\frac{\partial u}{\partial \chi} + \rho v\frac{\partial u}{\partial r} = G(1-\rho) + \frac{1}{r}\frac{\partial}{\partial r}\left(r\frac{\partial u}{\partial r}\right) \tag{2}$$

$$\rho u\frac{\partial Z}{\partial \chi} + \rho v\frac{\partial Z}{\partial r} = \frac{1}{Pr}\frac{1}{r}\frac{\partial}{\partial r}\left(r\frac{\partial Z}{\partial r}\right) \tag{3}$$

where $G = gL_d/U_0^2$, assumed to be of order unity, measures the buoyancy effects upstream of the flame front region. Here, $Z = (S\hat{Y}_F + 1 - \hat{Y}_0)/(S+1)$ stands for the mixture fraction, a conserved scalar with a value 1 in the fuel stream and 0 in the air stream. The reader should remember that the viscosity μ and ρD_T were considered to be functions only of the temperature, so that they are constant upstream of the flame front.

Because the mass diffusivities are equal, the reduced mass fractions $\hat{Y}_F = Y_F/Y_{F0}$ and $\hat{Y}_0 = Y_{0_2}/Y_{0_2 A}$ are given by

$$\hat{Y}_F = 1 - \hat{Y}_0 = Z, \tag{4}$$

while the mass fraction of nitrogen, considered to be the dilutant in the fuel stream, will be given by

$$Y_{N_2} = (1 - Y_{0_2 A})(1 - Z) + (1 - Y_{F0})Z. \tag{5}$$

With $T = T_0$, the equation of state gives the nondimensional value of the density ρ as

$$\rho = \frac{M}{M_A} = \left[\frac{Y_{0_2 A}}{32} + \frac{1 - Y_{0_2 A}}{28}\right] \Big/ \left[\frac{Y_F}{M_F} + \frac{Y_{0_2}}{32} + \frac{1 - Y_F - Y_{0_2}}{28}\right] \tag{6}$$

where M_F is the molecular mass of the pure fuel, and M_A is the mean molecular mass in the air stream. This last equation reduces to

$$\rho = (1 - Y_{0_2 A}/8)/[1 - ZY_{F0}(1 - 28/M_F) - (1 - Z)Y_{0_2 A}/8], \qquad (7)$$

where use is made of Eqs. (4) and (5) to express the density as a function of Z.

The system of Eqs. (1)–(3) and (7) are to be solved for $\chi > 0$ and $r \geq 0$ with the boundary conditions

$$\chi = 0: \begin{cases} r > 1: & u - U_A/U_0 = Z = 0 \\ r < 1: & u = Z = 1 \end{cases} \qquad (8)$$

and

$$r = 0: \quad v = \frac{\partial u}{\partial r} = \frac{\partial Z}{\partial r} = 0 \qquad (9)$$

$$r \to \infty: \quad u - U_A/U_0 \to 0, \quad Z \to 0. \qquad (10)$$

Note that for $r \to \infty$ the product $-r\rho v \to \phi(\chi)$, a function of χ that determines the mass entrainment rate of air per unit length according to $\phi 2\pi a U_0/Re$.

The important outcome of the numerical solution are the velocity and mixture fraction profiles $u(r, \chi)$ and $Z(r, \chi)$, which when evaluated at $\chi = \chi_f = x_f/(aRe)$ will provide us with the flow and concentration profiles, $\tilde{u}(r)$ and $\tilde{Z}(r)$, just upstream of the flame front region

$$\tilde{u} = u(r, \chi_f), \quad \tilde{Z} = Z(r, \chi_f), \qquad (11)$$

which depend on the parameters χ_f, U_A/U_0 and G, and are to be used as boundary conditions for the equations for the flame front region. Notice that the dependence on the Reynolds number of these profiles appears only through the nondimensional flame front distance to the injector, χ_f.

THE FLAME FRONT REGION

Our aim in this section is to describe the dynamics and the structure of the flame front region generated after ignition by an external source at some location in the jet developing region. The flame created, which at early times may be a nearly spherical flame, will be rapidly elongated

by the flow. We shall try to describe the structure and dynamics of the upstream part of the flame front, of size of order a, that when located at a station $x_f(t)$, of order L_d, will propagate downstream with a velocity $U_f = \mathrm{d}x_f/\mathrm{d}t$ relative to the injector. We can expect U_f to be of order S_L, when the flow velocity is also of order S_L. If the flame lies at the lift-off distance $x_f = x_l$, then $U_f = 0$. If at a given station U_f turns out to be negative, the front will propagate upstream relative to the injector; if positive, the front will propagate downstream.

In order to describe the flow in the flame front region we shall use a reference frame moving with the front. Because the fluid transient time, a/U_0, across the region is small compared with the time L_d/U_0 required to see changes in the upstream conditions encountered by the front, we can consider the flow structure as quasi-steady relative to the reference system. When $G = gL_d/U_0^2$ is of order unity, and x_f is of order L_d, the buoyancy effects will be important both upstream and downstream of the flame front but not in the flame front region of size a, where we expect the fluid accelerations, of order U_0^2/a, to be large compared with g.

The conservation equations will be written in nondimensional form using a as scale for the coordinates $X = (x - x_f)/a$ and $r = r'/a$, S_L for the two velocity components $U = u'/S_L$ and $v = v'/S_L$ and $\rho_A S_L^2$ for the pressure differences from the hydrostatic far-field value. The resulting nondimensional form of the system of conservation equations is

$$\frac{\partial}{\partial X}(\rho U) + \frac{1}{r}\frac{\partial}{\partial r}(\rho r V) = 0 \tag{12}$$

$$\rho U\frac{\partial U}{\partial X} + \rho V\frac{\partial U}{\partial r} = -\frac{\partial p'}{\partial X} + \frac{\delta_L}{a}Pr\left\{\frac{\partial}{\partial X}\left(2\mu\frac{\partial U}{\partial X}\right) + \frac{1}{r}\frac{\partial}{\partial r}\left[r\mu\left(\frac{\partial V}{\partial X} + \frac{\partial U}{\partial r}\right)\right]\right\} \tag{13}$$

$$\rho U\frac{\partial V}{\partial X} + \rho V\frac{\partial V}{\partial r} = -\frac{\partial p'}{\partial r} + \frac{\delta_L}{a}Pr\left\{\frac{\partial}{\partial X}\left[\mu\left(\frac{\partial V}{\partial X} + \frac{\partial U}{\partial r}\right)\right] + \frac{1}{r}\frac{\partial}{\partial r}\left(2\mu r\frac{\partial V}{\partial r}\right) - 2\mu\frac{V}{r^2}\right\} \tag{14}$$

$$\rho U\frac{\partial Z}{\partial X} + \rho V\frac{\partial Z}{\partial r} = \frac{\delta_L}{a}\left\{\frac{1}{r}\frac{\partial}{\partial r}\left(\rho D_T r\frac{\partial Z}{\partial r}\right) + \frac{\partial}{\partial X}\left(\rho D_T\frac{\partial Z}{\partial X}\right)\right\} \tag{15}$$

$$\rho U\frac{\partial \hat{Y}_F}{\partial X}+\rho V\frac{\partial \hat{Y}_F}{\partial r}=\frac{\delta_L}{a}\left\{\frac{1}{r}\frac{\partial}{\partial r}\left(\rho D_T r\frac{\partial \hat{Y}_F}{\partial r}\right)+\frac{\partial}{\partial X}\left(\rho D_T\frac{\partial \hat{Y}_F}{\partial X}\right)\right\}+\frac{a}{\delta_L}w_F \tag{16}$$

where the viscosity μ and the thermal diffusivity D_T are scaled with their values in the air stream. In the unity-Lewis-number approximation used here, the nitrogen mass fraction is given by Eq. (5), while the oxidizer mass fraction and the temperature are given by

$$Z=(S\hat{Y}_F+1-\hat{Y}_0)/(S+1) \tag{17}$$

and

$$(T-T_0)/(T_0\gamma)+\hat{Y}_F+\hat{Y}_0=1, \tag{18}$$

where $\gamma=(T_s-T_0)/T_0$ is the dimensionless stoichiometric temperature increase. These equations must be supplemented with the equation of state $\rho=(M/M_A)(T_0/T)$

$$\frac{M}{M_A}=\left[\frac{Y_{O_2A}}{32}+\frac{1-Y_{O_2A}}{28}\right]\Bigg/\left[\frac{Y_F}{M_F}+\frac{Y_{O_2}}{32}+\frac{Y_{N_2}}{28}+\frac{Y_P}{M_P}\right], \tag{19}$$

where M_P is the molecular mass of the products, whose local mass fraction is determined from $Y_P=1-Y_{O_2}-Y_F-Y_{N_2}$. The temperature dependence of the viscosity and thermal diffusivity will be described with a power law of the form $\mu=\rho D_T=(T/T_0)^\sigma$ with $\sigma=0.7$. The nondimensional reaction term $(a/S_L)W_F/\rho_A Y_{F0}$ has been written in the form $(a/\delta_L)w_F$ by measuring the overall reaction rate $W_F/(\rho Y_{F0})$ with its characteristic value $S_L/\delta_L=S_L^2/D_{TA}$, to obtain a nondimensional reaction rate w_F, of order unity in the premixed flame layers, which is a function of the temperature and the mass fractions. This is given below in Eq. (26) for an overall Arrhenius reaction.

The upstream boundary conditions to be used for the conservation equations are

$$U=-\frac{U_f}{S_L}+\frac{U_0}{S_L}\tilde{u}(r),\quad \hat{Y}_F=Z=\tilde{Z}(r)\quad \text{as}\quad X\to-\infty, \tag{20}$$

where $\tilde{u}(r)$ and $\tilde{Z}(r)$ depend on U_A/U_0, G and $\chi_f=x_f/(aRe)$, the parameter that defines the flame front location. In these conditions, derived from Eq. (11), the ratio U_0/S_L appears together with the front propagation velocity U_f/S_L, which is to be calculated. If we want to account

for the perturbation in the upstream-flow velocities that results from the effect of the thermal expansion in the flame front region, we should include the flow associated with a volumetric source of strength $b\pi a^2 S_L$, placed at $x = x_f$ and $r = 0$, with b, of order unity, to be calculated as part of the solution. However, these perturbations decay like X^{-2}, and are accounted for when computing the flame front region. Downstream, as $X \to \infty$, the solution will evolve to a flow that involves slow variations with X, associated with radial diffusion effects, which can be described using approximations of the boundary-layer type. Instead of using this asymptotic solution as the downstream boundary condition, when solving the system of Eqs. (12)–(16), a weak form of the boundary conditions, such as

$$\frac{\partial U}{\partial X} = \frac{\partial Z}{\partial X} = \frac{\partial \hat{Y}_F}{\partial X} = 0 \quad \text{as} \quad X \to \infty, \tag{21}$$

can be employed for simplicity. In addition, the symmetry conditions given in Eq. (9) hold at $r = 0$, while

$$U + (U_f - U_A)/S_L \to 0, \quad \hat{Y}_F \to 0 \quad \text{and} \quad Z \to 0 \quad \text{as} \quad r \to \infty \tag{22}$$

To complete the boundary conditions, we must add a condition linking the origin of the coordinate system to the flame front.

We must stress here that our formulation is dependent on the separation in domains of the flow field, which is justified for large values of the ratio, $L_d/a = Re$, of the scales L_d, of the nonreacting region of the jet, and a, of the flame front region. The ratio $a/\delta_L = aS_L/D_{TA}$ appearing in Eqs. (12)–(16), of the order of the Reynolds number $Re = U_0 a/\nu_A$, is a large number. As a result, the viscous and diffusion terms, as well as the reaction term, are nonnegligible only in a thin reaction layer, the curved premixed flame with its rich and lean branches, of thickness δ_L small compared with a. The flow in the flame front region outside this thin flame is inviscid; and for this reason the upstream boundary conditions given in Eq. (20) are meaningful. Then, aside from jumps across the premixed flames, the temperature and the mass fractions remain constant along the streamlines, which are nonparallel due to the thermal expansion effects. In the limit $a/\delta_L \gg 1$, one could in principle solve the flow in the flame front region by considering the flame as a curved reaction sheet embedded in the inviscid flow region, but the numerical solution of the resulting free boundary problem is anticipated to be

complex. The alternative approach proposed here, and used by Ruetsch et al. (1995), involves the integration of Eqs. (12)–(16) for large values of a/δ_L. The results, and in particular the value for the front velocity U_f/S_L, will be weakly dependent on a/δ_L when sufficiently large values are considered. The structure of the resulting flame front is locally planar, with small relative errors of order $\delta_L/a \ll 1$. Correspondingly, at a given radial location the flame propagates with respect to the local incoming flow with a velocity equal to that of a planar flame, which is a function of the local equivalence ratio $\phi = SZ/(1-Z)$ encountered by the flame. This variation of the planar-flame velocity with ϕ enters as the essential ingredient of the influence of the kinetics on the flame front structure.

A number of parameters appear in the formulation above, including the parameters, U_A/U_0 and G, characterizing the flow velocity field upstream of the flame front region, together with the nondimensional flame front distance $\chi_f = x_f/(aRe)$, and the nondimensional values U_0/S_L and U_f/S_L of the initial fuel velocity and the front velocity, to be calculated as an eigenvalue. In the conservation equations for the flame front region we find the parameter γ characterizing the exothermicity of the reaction, and the stoichiometric parameter S, in addition to Pr and the Peclet number $a/\delta_L = aS_L/D_{TA}$, based on S_L and the initial air thermal diffusivity. The nondimensional front velocity

$$U_f/S_L = F(\chi_f, U_0/S_L, U_A/U_0, G, S, \gamma, Pr, a/\delta_L) \tag{23}$$

which appears in Eqs. (20) and (22) must be calculated as an eigenvalue as part of the solution for given values of these parameters.

To complete the problem formulation, one needs to provide an expression for the fuel consumption rate. One could for instance incorporate detailed kinetics in the computation, as done by Plessing et al. (1998), but such an approach, which is computationally expensive, is not strictly necessary. As explained above, in the limit $a/\delta_L \gg 1$ considered here the flame front is locally planar, so that the results should not be very dependent on the model adopted for the chemical kinetics, provided that the selected rate law W_F be able to describe the variations of the planar flame propagation velocity with the equivalence ratio. Therefore, an overall reaction can be considered, the simplest example being an Arrhenius kinetic expression of the form

$$W_F/(\rho Y_{F0}) = -B\hat{Y}_F\hat{Y}_0 \exp[-E/(RT)] \tag{24}$$

involving a frequency factor B and an activation energy E. This last expression can be scaled with

$$\frac{S_L^2}{D_{TA}} = \frac{4B}{\beta^3}\left(\frac{T_s}{T_0}\right)^{\sigma-1}\frac{S}{S+1}\exp\left[-\frac{E}{RT_s}\right], \tag{25}$$

corresponding to the asymptotic expression of the stoichiometric planar flame velocity, to give

$$w_F = -\frac{\beta^3}{4}\left(\frac{T_s}{T_0}\right)^{1-\sigma}\frac{S+1}{S}\hat{Y}_F\hat{Y}_0\exp\left[\frac{E}{RT_s}\frac{(T-T_s)}{T}\right], \tag{26}$$

where changes in the mean molecular mass and in the difference of the Lewis number from unity are neglected when writing Eq. (25). In this simple Arrhenius law, the Zeldovich number $\beta = E(T_s - T_0)/(RT_s^2)$, which is typically large, embodies the dependence of the flame propagation velocity on ϕ. Modifications to Eq. (26) are in general needed for an accurate description of this dependence, including for instance reaction orders different from unity for both fuel and oxidizer (Westbrook and Dryer, 1981). However, we have chosen in the calculations presented below the approach recently adopted by Garrido-López and Sarkar (2004), following a suggestion of Forman Williams, of considering a variable activation energy, selected as a function of the local equivalence ratio ϕ to mimic the dependence on ϕ of the planar flame velocity.

The main result of the computation outlined above is the front propagation velocity U_f with respect to the injector. It is worth pointing out that most of the previous numerical and theoretical studies considered instead the front propagation velocity relative to the incoming flow along the stoichiometric surface; but such an approach is only strictly appropriate when the incoming flow has a uniform velocity profile, i.e., for $U_0 = U_A$. In the formulation considered here, positive values of U_f correspond to fronts convected downstream, while negative values are associated with fronts moving upstream toward the injector. On the other hand, when $U_f = 0$ the front location $\chi_f = \chi_l$ corresponds to the lift-off distance from the injector

$$\chi_l = \chi_l(U_0/S_L, U_A/U_0, G, S, Pr, \gamma), \tag{27}$$

whose parametric dependence on the Peclet number a/δ_L can be neglected in the first approximation.

The Lewis numbers, considered equal to unity in the presentation of this paper, will also play a role in defining the lift-off distance, as shown by Lee and Chung (1997).

LIMITING FORMULATIONS AND PRELIMINARY RESULTS

The above formulation for the flame front region is derived in the distinguished limit $S \sim 1$, as corresponds to diluted fuel feed, with U_0/S_L and U_A/U_0 also taken to be of order unity. When undiluted fuel feed is considered, S takes large values (e.g., $S \simeq 17.4$ for methane-air combustion), so that the limit $S \gg 1$ deserves separate attention. In particular, it is of interest to describe the nonreacting concentration field, when $S \gg 1$, that we encounter for $U_A/U_0 \ll 1$. In this case, stoichiometric conditions and the flame can be found at large distances from the jet exit of order $S\,a\,Re$, much larger than the jet development region, where the jet velocity has decreased to small values of order $S^{-1}U_0$; clearly, the flame lies in this far-field region if $S^{-1}U_0 \sim S_L$. As explained by Revuelta et al. (2002), the description of the mixing process taking place upstream from the flame is simplified if the condition $U_A/U_0 \ll S^{-1}$ is satisfied, when the velocity and mixture fraction fields are given by the self-similar Schlichting-Squire solution in the absence of gravity effects. The effects of gravity should be retained there if S^2G is of order unity or larger. On the other hand, in the distinguished limit $U_A/U_0 \sim S^{-1}$, the coflow velocity is of the order of the axial velocity for $x \sim S\,a\,Re$, and the boundary-layer Eqs. (1)–(3), written in terms of the rescaled variables of order unity χ/S, r/S, Su, Sv and SZ, need to be integrated numerically to describe the nonreacting jet. Note that modified coordinates r/S and $(x - x_f)/(Sa)$ also need to be introduced in the formulation of the flame front region. The resulting nondimensional front velocity U_f/S_L will be a function of the nondimensional flame front distance $x_f/(S\,a\,Re)$, the kinetic parameter $U_0/(S\,S_L)$, the buoyancy parameter $G\,S^2$, the nondimensional coflow velocity $U_A\,S/U_0$, and the exothermicity parameter γ.

The Damköhler number $(a/\delta_L)^2$, defined as the ratio of the diffusion time, a^2/D_{TA}, and the chemical time, δ_L^2/D_{TA}, in jet diffusion flames lifted to a distance of the order $L_d = a\,Re$, is large enough to eliminate its influence on the flame front velocity and on the lift-off distance. However, when for the lower values of U_0/S_L the flame front distance is small compared with L_d, the front lies in this case in the annular mixing layer that originates at the injector rim. This has a local thickness

$\delta_m = (D_{TA}x/U_0)^{1/2} \ll a$, and it is planar in first approximation. Therefore we shall present in the following some results of the numerical description of the flame front lifted at these distances small compared with L_d. In this case the relevant Damköhler number $(\delta_m/\delta_L)^2$ is much lower than $(a/\delta_L)^2$ so that its effect on U_f/S_L becomes important.

If we neglect buoyancy effects, considering distances $x \ll U_0^2/g$, a self-similar description is available for the nonreacting mixing layer, with the velocity $u(\eta)$ and mixture fraction $Z(\eta)$ given in terms of the similarity variable $\eta = y/(D_{TA}x/U_0)^{1/2}$, where $y = r - 1$. Introducing a similarity stream function $F(\eta)$ defined from $\psi = \rho_A U_0 (D_{TA}x/U_0)^{1/2} F$, reduces the problem given in Eqs. (1)–(3) to that of integrating

$$Pr\frac{d^2u}{d\eta^2} + \frac{1}{2}F\frac{du}{d\eta} = 0 \tag{28}$$

$$\frac{d^2Z}{d\eta^2} + \frac{1}{2}F\frac{dZ}{d\eta} = 0 \tag{29}$$

with $\rho u = dF/d\eta$ and with boundary conditions $dF/d\eta \to U_A/U_0$ and $Z \to 0$ as $\eta \to \infty$ and $dF/d\eta \to M_F/M_A$ and $Z \to 1$ as $\eta \to -\infty$. At the flame location $x = x_f$ the mixing layer has a thickness $\delta_m = (D_{TA}x_f/U_0)^{1/2}$, so that the velocity and mixture fraction are given by $\tilde{u} = u(y/\delta_m)$ and $\tilde{Z} = Z(y/\delta_m)$. These distributions are to be used in the boundary conditions when integrating the conservation equations in the flame front region, which need to be written in terms of the coordinates y/δ_m and $(x - x_f)/\delta_m$, and terms of order δ_m/a representing curvature effects can be neglected. The flame front distance χ_f and the kinetic parameter a/δ_L are replaced in the resulting formulation by the Damköhler number $Da = (\delta_m/\delta_L)^2 \gg 1$, with U_0/S_L, U_A/U_0 and S appearing as additional parameters.

Triple flames in planar mixing layers have been computed in a number of previous investigations, which were restricted to values of S of order unity (Ruetsch et al., 1995; Plessing et al., 1998; Walsh et al., 2004). We present in Figure 2 results obtained for undiluted fuel feed ($S \gg 1$). The results correspond to equal velocities of fuel and oxidizer, $U_A/U_0 = 1$, for which a uniform velocity profile $u' = U_0$ is found upstream from the flame front region. The computation provides in this case the front velocity relative to the upstream flow $U_f' = -U_f + U_0$, which is computed with an Arrhenius law for the fuel consumption rate.

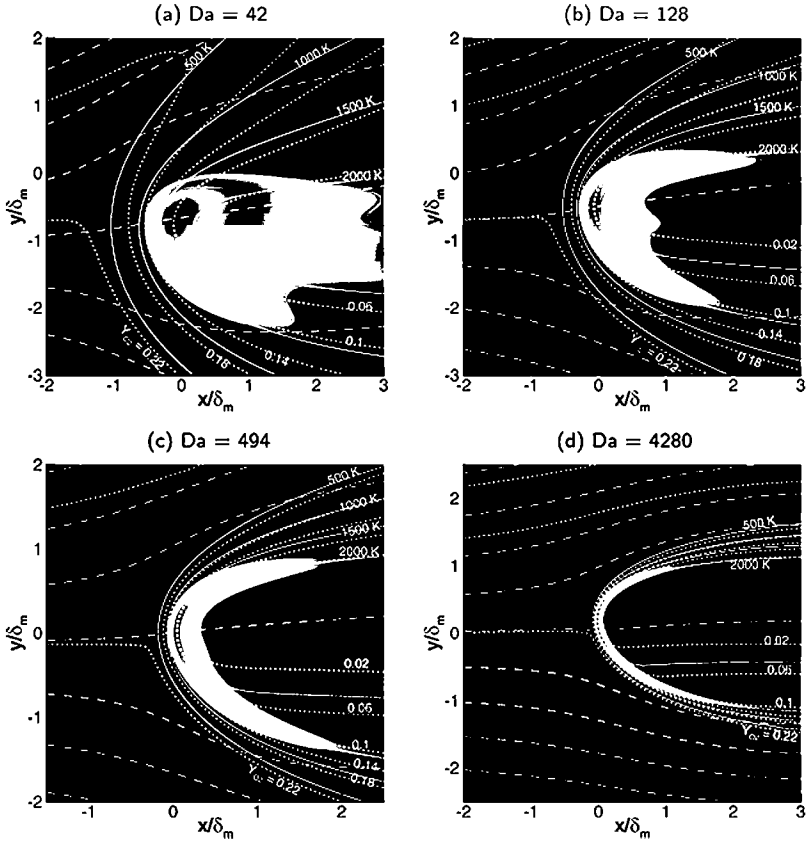

Figure 2. Structure of the solution for undiluted fuel ($Y_{CH_4F} = 1$) and different Damköhler numbers, $Da = (\delta_m/\delta_L)^2$, when the flame is lifted off far away from the injector rim. Figures (*a*), (*b*), (*c*), and (*d*) correspond respectively to points labeled a, b, c, and d in Figure 3. Solid lines: contours of temperature from $T = 500\,\mathrm{K}$ to $T = 2000\,\mathrm{K}$ at intervals $\Delta T = 500\,\mathrm{K}$. Dashed lines: streamlines at intervals $\Delta\psi = 0.5\,\rho_s\,U_0\,\delta_m$. Dotted lines: contours of oxygen mass fraction from 0.22 to 0.02 at intervals $\Delta Y_{O_2} = 0.04$. The reaction rate is shown in colors for illustrative purposes. (See Color Plate 1 at the end of this issue).

The resulting nondimensional propagation velocity U_f'/S_L is a function of the exothermicity parameter γ, the fuel-to-air stoichiometric ratio S, the Damköhler number $Da = (\delta_m/\delta_L)^2$, and the Zeldovich number β. Methane-air combustion is considered, giving $\gamma = 6.7$ and $S = 17.4$. For improved accuracy, the activation energy is varied with the local equivalence ratio $\phi = SZ/(1 - Z)$ according to $E/E_0 = 1 + 2(0.7 - \phi)^2$

for $\phi \leq 0.7$, $E/E_0 = 1$ for $0.7 \leq \phi \leq 1.0$, and $E/E_0 = 1 + 1.472(\phi - 1)^2$ for $1.0 \leq \phi$ with $E_0 = 125000\,\mathrm{J/(mol\ K)}$. With this law, the Arrhenius overall reaction is able to reproduce with small errors the planar flame propagation velocity within the flammability limits. Note that the Zeldovich number based on E_0, $\beta = E_0(T_s - T_0)/(RT_s^2) = 5.7$, is moderately large.

Figure 2 shows the flame front structure for four different values of the Damköhler number, $Da = (\delta_m/\delta_L)^2$. The range of Da selected in the figure allows us to see the evolution of the flame front from an edge flame for sufficiently small Da to a thin premixed front with a negligibly weak trailing diffusion flame for $Da \to \infty$. For $\beta \gg 1$, the transition from edge flames to triple flames should occur when the more relevant value of the Damköhler number $[\delta_m/(\beta\delta_L)]^2$, based on the size δ_m/β of the flame front region, increases above 1. Notice that $\delta_m/(\beta\delta_L)$ is also the ratio of the burning rate per unit flame surface in the premixed and in the diffusion flames, so that for large values of the Damköhler number the contributions of the burning rate in the diffusion flame cease to be visible.

The propagation velocity U_f'/S_L of the front with respect to the upstream flow is shown in Figure 3 as a function of the local Damköhler

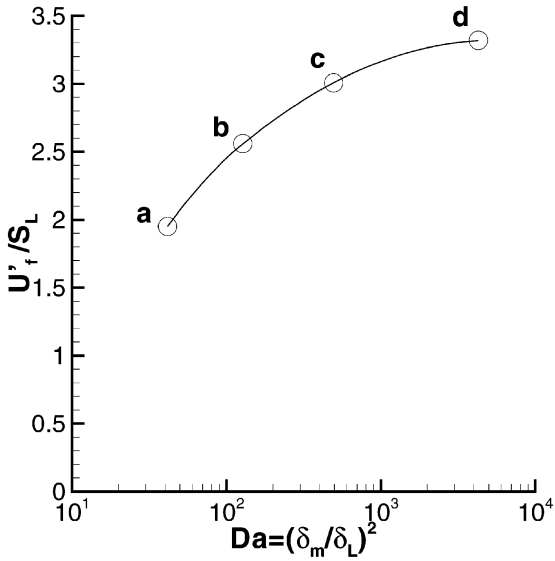

Figure 3. The variation of the nondimensional flame front velocity relative to the injector U_f'/S_L with the Damköhler number, $Da = (\delta_m/\delta_L)^2 = D_{TA}x_f/U_0\delta_L^2$.

number $(\delta_m/\delta_L)^2 = D_{TA}\, x_f/U_0\, \delta_L^2$. As can be seen, for sufficiently large values of Da the velocity becomes weakly dependent on Da. The extrapolation of the results indicates that the asymptotic value $U_f'/S_L = 3.46$ is approached as $Da \to \infty$. This limiting value is associated with critical conditions for blow-off in planar mixing layers, a result in agreement with previous experimental observations (Muñiz and Mungal, 1997).

We can use Figure 3 to calculate the lift-off distance x_l for a given flow velocity U_0 by equating U_f'/S_L to U_0/S_L. Notice that due to the growth of U_f'/S_L with x_f the resulting position of the flame front is stable. For values of U_0/S_L smaller than the blow-off value $(U_0/S_L)_b = 3.46$ the flame will remain lifted.

We can anticipate that the results will be applicable to other fuels not strongly diluted, having values of γ close to that of methane, and with large values of S.

CONCLUDING REMARKS

We have given in this paper the formulation required for the numerical description of the quasi-steady propagation of laminar flame fronts in round jets, which includes as a particular case the description of lifted diffusion flames. The analysis exploits the disparity of scales appearing for moderately large values of the Reynolds number. The formulation given incorporates variations of density and transport coefficients with temperature and composition. A realistic model for the fuel consumption rate, able to describe the variation with the equivalence ratio of the propagation velocity of planar flames, must be employed for an accurate computation of flame front velocities. The formulation can be used in future work for the numerical analysis of the structure and dynamics of laminar flame fronts. Although some illustrative examples are presented here, much remains to be done in the field.

REFERENCES

Aggarwal, S.K., Puri, I.K., and Qin, X. (2001) A numerical and experimental investigation of "inverse" triple flames. *Phys. Fluids*, **13**, 265–275.

Azzoni, R., Ratti, S., Aggarwal, S.K., and Puri, I.K. (1999) The structure of triple flames stabilized on a slot burner. *Combust. Flame*, **119**, 23–40.

Boulanger, J. and Vervisch, L. (2003) Effects of heat release in laminar diffusion flames lifted in round jets. *Combust. Flame*, **134**, 355–368.

Buckmaster, J. (1996) Edge flames and their stability. *Combust. Sci. Technol.*, **115**, 41–68.

Buckmaster, J. (2002) Edge-flames. *Prog. Energy Combust. Sci.*, **28**, 435–475.

Buckmaster, J. and Matalon, M. (1988) Anomalous Lewis number effects in tribrachial flames. *Proc. Combust. Inst.*, **22**, 1527–1535.

Buckmaster, J. and Weber, R. (1996) Edge-flame holding. *Proc. Combust. Inst.*, **26**, 1143–1149.

Chung, S.H. and Lee, B.J. (1991) On the characteristics of laminar lifted flames in a nonpremixed jet. *Combust. Flame*, **86**, 62–72.

Daou, J. and Liñán, A. (1998) The role of unequal diffusivities in ignition and extinction fronts in strained mixing layers. *Combust. Theory Model.*, **2**, 449–477.

Dold, J.W. (1989) Flame propagation in a nonuniform mixture: Analysis of a slowly varying triple flame. *Combust. Flame*, **76**, 71–88.

Dold, J.W., Hartley, L.J., and Green, D. (1991) Dynamics of laminar triple-flamelet structures in non-premixed turbulent combustion. In Fife, P.C., Liñán, A., and Williams, F. (Eds.) *Dynamical Issues in Combustion Theory, IMA Volumes in Mathematics and its Applications*, Springer-Verlag, New York, pp. 83–105.

Favier, V. and Vervisch, L. (1998) Investigating the effects of edge flames in lift-off in non-premixed turbulent combustion. *Proc. Combust. Inst.*, **27**, 1239–1245.

Favier, V. and Vervisch, L. (2001) Edge flames and partially premixed combustion in diffusion flame quenching. *Combust. Flame*, **125**, 788–803.

Fernández, E., Kurdyumov, V., and Liñán, A. (2000) Diffusion flame attachment and lift-off in the near wake of a fuel injector. *Proc. Combust. Inst.*, **28**, 2125–2131.

Garrido-López, D. and Sarkar, S. (2004) Effects of imperfect premixing coupled with hydrodynamic instability on flame propagation. *Proc. Combust. Inst.*, **30**, (in press).

Ghosal, S. and Vervisch, L. (2000) Theoretical and numerical study of a symmetrical triple flame using the parabolic flame path approximation. *J. Fluid Mech.*, **415**, 227–260.

Hartley, L.J. and Dold, J.W. (1991) Flame propagation in a nonuniform mixture: Analysis of a triple flame. *Combust. Sci. Technol.*, **80**, 23–46.

Kioni, P.N., Rogg, B., Bray, K.N.C., and Liñán, A. (1993) Flame spread in laminar mixing layers: The triple flame. *Combust. Flame*, **95**, 276–290.

Lee, B.J. and Chung, S.H. (1997) Stabilization of lifted tribrachial flames in a laminar nonpremixed jet. *Combust. Flame*, **109**, 163–172.

Liñán, A. (1988) Diffusion flame attachement and flame front propagation along mixing layers. In Brauner, C.F. and Schmidt-Lain, C. (Eds.) *NATO ASI Series E*, **140**, Martinus Nijhoff, The Netherlands, pp. 151–154.

Liñán, A. (1994) Ignition and flame spread in laminar mixing layers. In Buckmaster, J., Jackson, T.L., and Kumar, A. (Eds.) *Combustion in High-Speed Flows*, Kluwer Academic Publications, Dordrecht (The Netherlands), pp. 461–476.

Liñán, A. and Crespo, A. (1976) An asymptotic analysis of unsteady diffusion flames for large activation energies. *Combust. Sci. Technol.*, **14**, 95–117.

Mizobuchi, Y., Tachibana, S., Shinio, J., Ogawa, S., and Takeno, T. (2002) A numerical analysis of the structure of a turbulent hydrogen jet lifted flame. *Proc. Combust. Inst.*, **29**, 2009–2015.

Muñiz, L. and Mungal, M.G. (1997) Instantaneous flame-stabilization velocities in lifted-jet diffusion flames. *Combust. Flame*, **111**, 16–31.

Nayagam, V. and Williams, F.A. (2002) Lewis-number effects on edge-flame propagation. *J. Fluid Mech.*, **458**, 219–228.

Phillips, H. (1965) Flame in a buoyant methane layer. *Proc. Combust. Inst.*, **10**, 1277–1283.

Peters, N. (1986) Laminar flamelet concepts in turbulent combustion. *Proc. Combust. Inst.*, **21**, 1231–1250.

Peters, N. (2000) Turbulent Combustion, Cambridge University Press, Cambridge.

Plessing, T., Terhoeven, P., Peters, N., and Mansour, M.S. (1998) An experimental and numerical study of a laminar triple flame. *Combust. Flame*, **115**, 335–353.

Réveillon, J., Domingo, P., and Vervisch, L. (1995) Non-premixed flame ignition in turbulent flows, triple flames. In *Tenth Symposium on Turbulent Shear Flows*, University Park, PA, pp. 14–16.

Revuelta, A., Sánchez, A.L., and Liñán, A. (2002) Laminar mixing in diluted and undiluted fuel jets upstream from lifted flames. *Combust. Flame*, **128**, 199–210.

Ruetsch, G.R., Vervisch, L., and Liñán, A. (1995) Effects of heat release on triple flames. *Phys. Fluids*, **7**, 1447–1454.

Santoro, V.S., Liñán, A., and Gomez, A. (2000) Propagation of edge flames in counterflow mixing layers: Experiments and theory. *Proc. Combust. Inst.*, **28**, 2039–2046.

Shay, M.L. and Ronney, P.D. (1998) Nonpremixed edge flames in spatially varying straining flows. *Combust. Flame*, **112**, 171–180.

Smith, G., Golden, D., Frenklach, M., Moriarty, N., Eiteneer, B., Goldenberg, M., Bowman, T., Hanson, R., Song, S., Gardiner, Jr., W., Lissianski, V., and Qin, Z. (1999) GRI-Mech. http://www.me.berkeley.edu/gri_mech/.

Smooke, M.D. and Giovangigli, V. (1990) Formulation of the premixed and nonpremixed test problems. In Smooke, M.D. (Ed.) *Reduced Kinetic Mechanisms and Asymptotic Approximations for Methane-Air Flames*, Springer-Verlag, New York, pp. 1–28.

Takahashi, F. and Katta, V.R. (1990) Lifting criteria of jet diffusion flames. *Proc. Combust. Inst.*, **23**, 677–683.

Takahashi, F., Schmoll, W.J., and Katta, V.R. (1998) Attachment mechanisms of diffusion flames. *Proc. Combust. Inst.*, **27**, 675–684.

Vervisch, L. and Poinsot, T. (1998) Direct numerical simulation of non-premixed turbulent flames. *Annu. Rev. Fluid Mech.*, **30**, 655–692.

Westbrook, C.K. and Dryer, F.L. (1981) Simplified reaction mechanisms for the oxidation of hydrocarbon fuels in flames. *Combust. Sci. Technol.*, **27**, 31–43.

Walsh, K.T., Fielding, J., Smooke, M.D., Long, M.B., and Liñán, A. (2004) A comparison of computational and experimental lift-off heights of coflow laminar diffusion flames. *Proc. Combust. Inst.*, **30** (in press).

Williams, F.A. (1971) Theory of combustion in laminar flows. *Annu. Rev. Fluid Mech.*, **3**, 171–188.